Electronic Supplementary Material (ESI) for Journal of Materials Chemistry C.

Carbon nanotube fibers with martensite and austenite Fe residual catalyst: room temperature ferromagnetism and implications for CVD growth

B. Alemán[a], R. Ranchal[b], V. Reguero[a], B. Mas[a] and J. J. Vilatela[a,*]

[a]*IMDEA Materials Institute, Eric kandel 2, 28906 – Getafe, Madrid, Spain*

[b]*Dep, Física de Materiales, Universidad Complutense de Madrid, 28040 – Madrid, Spain*

Samples:

Four types of samples studied in this work. They consisted of fibers with different type of constituent CNTs (SWCNT or MWCNT), both types produced with a choice of Sulphur or Selenium. They are labelled S1 and S2 for sulphur, and SE1 and SE for selenium, respectively.

S1. Hysteresis loops

We performed an exhaustive magnetic characterization on representative fibers to exclude spurious effects in the magnetic results. At room temperature, the hysteresis loops of different pieces of fibers were measured in two different magnetometers (SQUID and VSM) also with different sample holders (Figure S1.a). The same magnetization curve is obtained in the different pieces of the same sample with both experimental set-ups, indicating that the magnetic signal is not due to spurious effects coming from the magnetometers, sample holders or the sample mounting process.

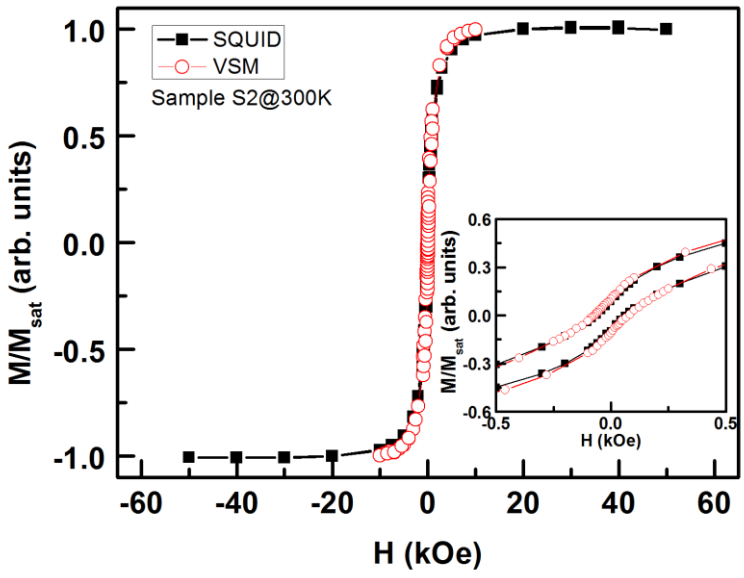

Figure S1.a. Room temperature hysteresis loops of a S-CNT fiber recorded in a SQUID and a VSM magnetometer, confirming that the room temperature ferromagnetism is produced by the fiber ruling out other possible ferromagnetic sources.

Figures S1.b and S1.c show the hysteresis loops of the CNT fibers produced with different promoters at 10K and RT respectively. The data shows that ferromagnetism is preserved within this temperature range.

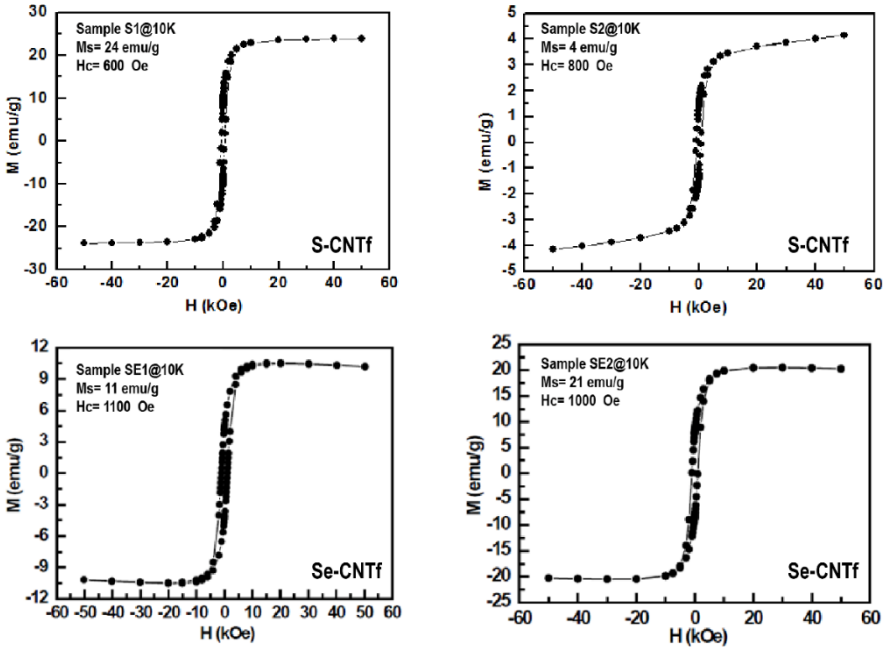

Figure S1.b. Hysteresis loops at 10 K of S- and Se-CNTf samples.

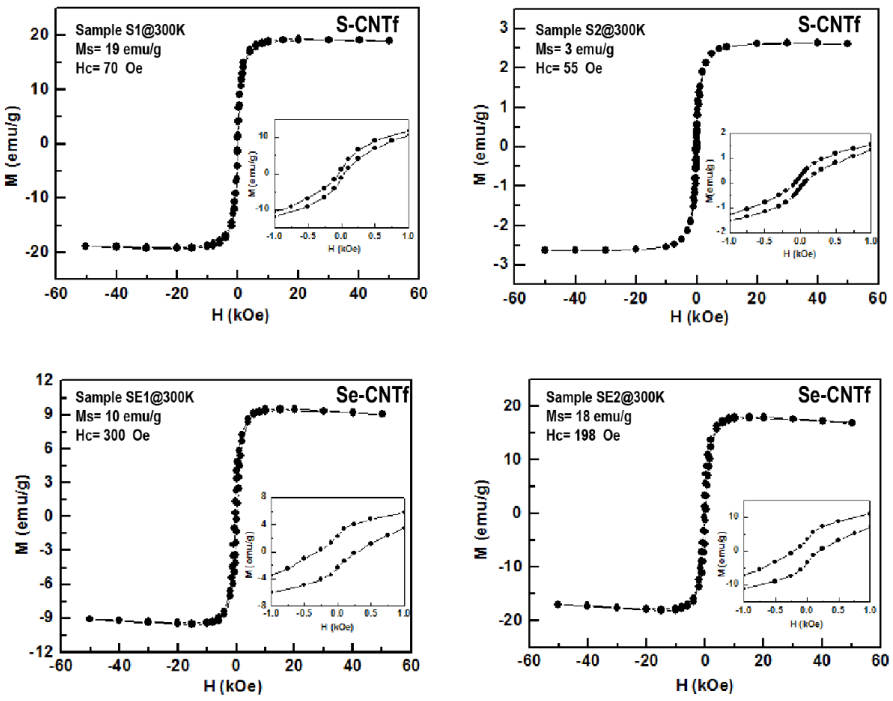

Figure S1.c. Hysteresis loops at 300 K of S- and Se-CNTf samples.

S2. Thermogravimetric analysis.

Through TGA we calculated Fe wt. % present in the fibers assuming that the residual materials after combustion corresponds to iron oxide (Fe_2O_3) (Figure S2 and Table S2).

Sample	**S-CNTf**		**Se-CNTf**	
	S1	S2	SE1	SE2
Residual				
Fe_2O_3 wt.%	20	5	10	7
Fe wt.%	15	4	8	6

Table S2. TGA residual wt. % and its corresponding Fe wt. %

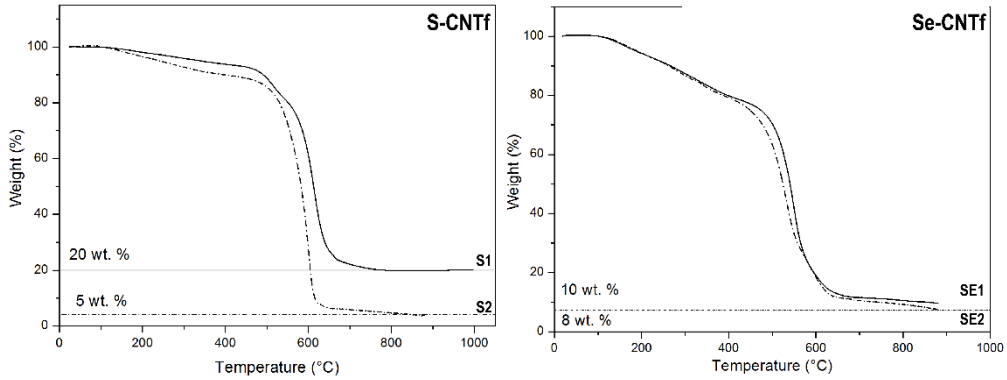

Figure S2. TGA curves showing residual wt. % for S- and Se-CNTf samples

S3. Field Cooling- Zero Field Cooling (FC-ZF) curves

Figure S3 shows the FC-ZFC curves of S- and Se-CNTf samples confirming a ferromagnetic behavior for all cases. Blocking temperature T_B is present at 140 K and above room temperature for S- and Se-CNTf samples respectively.

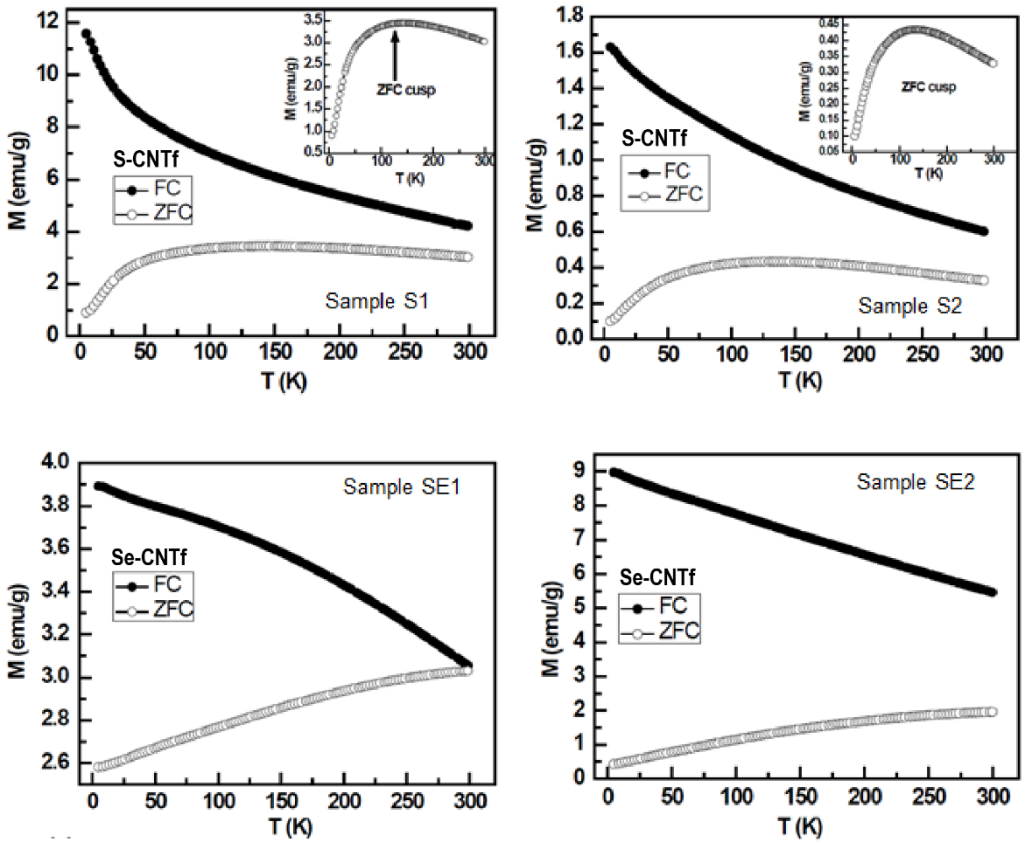

Figure S3. FC-ZFC curves of S- and Se-CNTf samples.

S4. Nanoparticle diameter dependence with blocking temperature

Theoretical nanoparticle size with d diameter is related to blocking temperature T_B through the equation:

$$KV = k_B T_B$$

$$V \equiv particle\ volume = \frac{\pi}{6} d^3$$

Considering BCC Fe magnetic anisotropy constant $K_{Fe\_BCC} = 4.18 \times 10^4\ J/m^3$ and Boltzmann constant $k_B = 1.38 \times 10^{-23}\ J/K$, we can express the nanoparticle diameter dependence with T_B as (Figure S4):

$$d(nm) = 0.9\, T_B^{1/3}$$

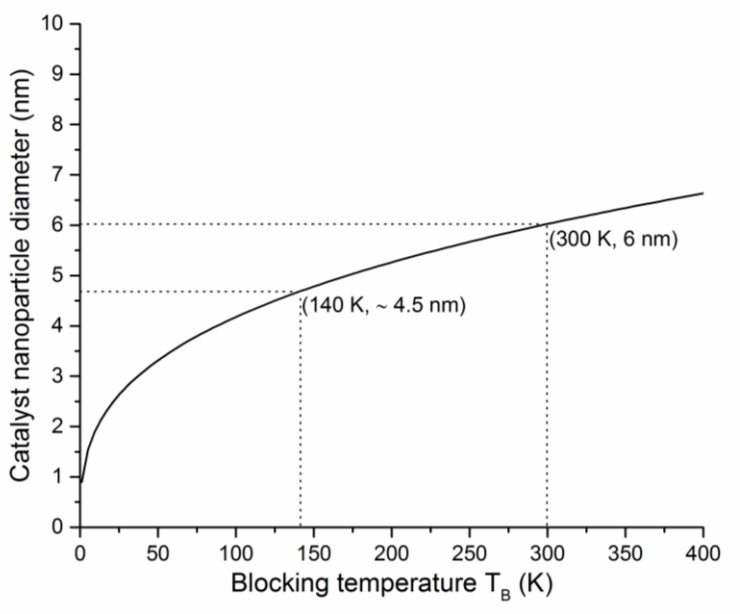

Figure S4.a. Catalyst nanoparticle diameter dependence with blocking temperature.

S5. Carbon mass dependence with catalyst nanoparticle critical diameter

In a catalyst nanoparticle with d diameter the carbon mass needed to produce a graphitic layer is $m_C=\pi \nu_C d^2$ (ν_C=*areal density of graphene sheet*=$0.75\cdot10^{-6}$ *kg/m*^{2}) while the mass of Fe in the particle is $m_{Fe}= (\pi/6)\rho_{Fe}d^3$ (ρ_{Fe}=*FCC Fe density*= 7.84 *g/cm*^{3}). Therefore we consider that taking into account the whole mass of the catalyst particle, the mass of carbon needed in order to generate a graphitic layer depends on the nanoparticle diameter as (Figure S5.a):

$$\frac{m_C}{m_C + m_{Fe}} \sim \frac{1}{2d+1}$$

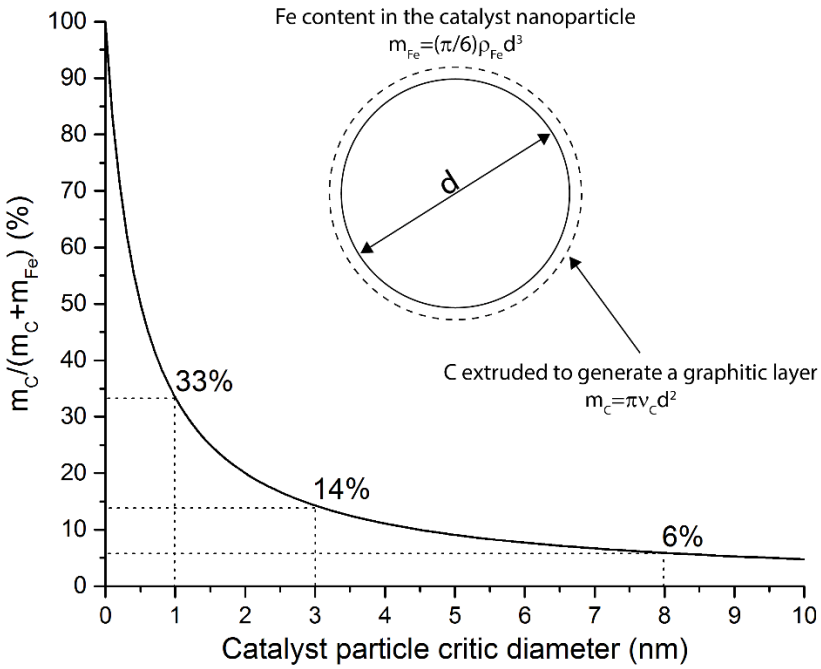

Figure S5.a. Catalyst particle carbon content dependence with the critic diameter of the nanoparticle in order to generate a graphitic layer.

Considering that the residual amount of C in an encapsulated catalyst nanoparticle is established by the critical diameter, we estimated the initial amount of C of a liquid nanoparticle (Figure S5.b) before cooling down through the following steps:

1) We consider catalyst critical diameter as 6 nm (average value of the nanoparticles studied in this work), so the final amount of C in the nanoparticle is 8 wt.%.
2) We know that post-growth encapsulated catalysts present a constant diameter to number of layers ratio around 3 (*d/#layers~3*), so nanoparticles of 6 nm diameter present an average of 2 layers.
3) If the catalyst is encapsulated with 2 graphitic layers we can estimate the whole C content considering the final amount of C (8 wt. %) and the C of the 2 layers ($m_C=\pi v_C d^2$), what gives an initial 26 wt. % of C in the liquid nanoparticle.
4) The mass of Fe remains constant during the process ($m_{Fe}= (\pi/6)\rho_{Fe}d^3= 9\cdot10^{-19}$ *g*).

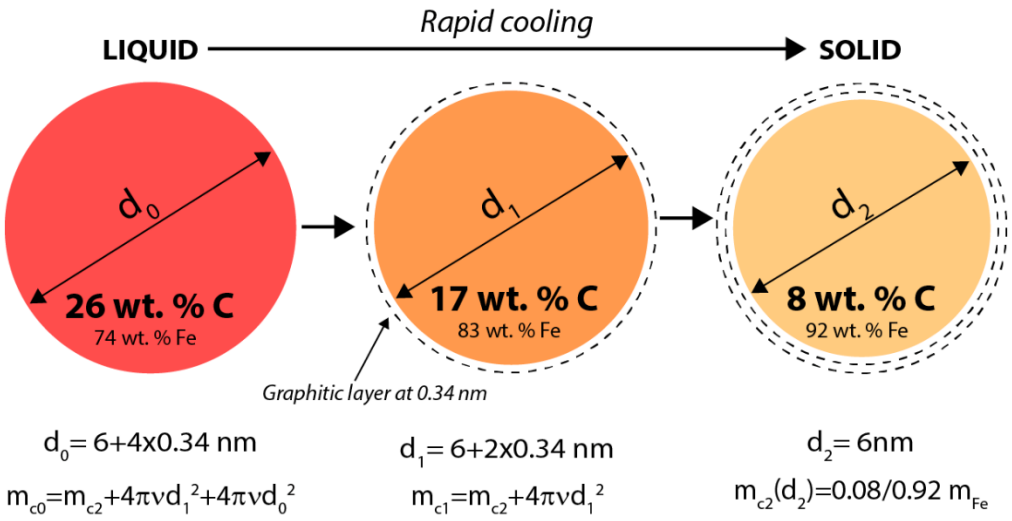

Figure S5.b. Estimation of the initial C content of a catalyst particle in the liquid state from its final solid state represented by a nanoparticle with a critic diameter of 6nm encapsulated by 2 graphitic layers.

S6. Austenitic (FCC), martensitic (BCT) and ferritic (BCC) crystal structures in Fe-C systems

Figure S6.a shows the austenitic FCC Fe crystal structure with $a_{FCC}=3.6$ Å lattice parameter and its corresponding BCT structure with $a'_{FCC}=3.6/\sqrt{2}$ Å and $c'_{FCC}=3.6$ Å lattice parameters. Compared to austenitic FCC Fe, martensitic structure presents an expansion along *a* axis and a contraction along *c* axis as the crystal structure of Figure S6.b shows with $a_{BCT}=2.86$ Å and $c_{BCT}=2.96$ Å. In absence of carbon, the most stable crystal structure at room temperature is ferritic BCC Fe (Figure S6.c) with $a_{BCC}=2.86$ Å lattice parameter.

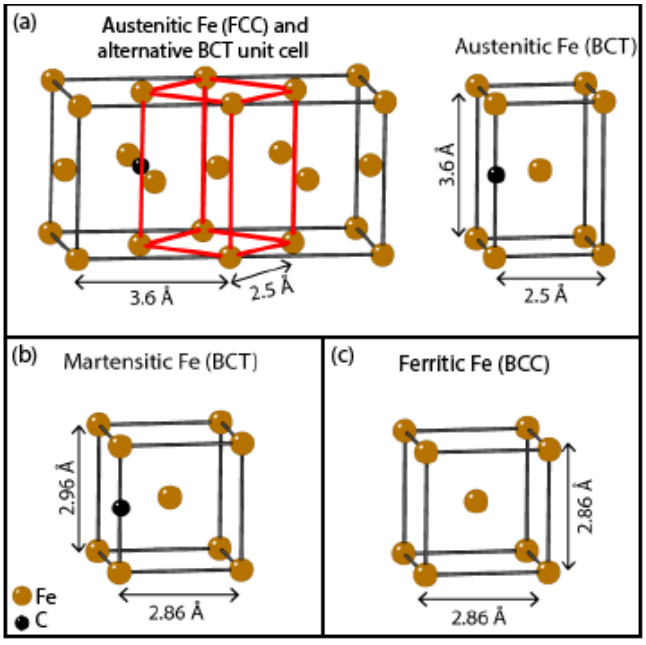

Figure S6. (a) Austenitic FCC Fe and its corresponding alternative BCT unit cell, (b) martensitic BCT Fe and (c) ferritic BCC Fe.